Woidy, P.; Karttunen, A.J.; Widenmeyer, M.; Niewa, R.; Kraus, F.

On Copper(I)-Fluorides, the Cuprophilic Interaction, the Preparation of Copper Nitride at Room Temperature, and the Formation Mechanism at Elevated Temperatures

Published in:
CHEMISTRY: A EUROPEAN JOURNAL

DOI:
10.1002/chem.201406136

Published: 01/01/2015

Document Version
Early version, also known as pre-print

Please cite the original version:
Woidy, P., Karttunen, A. J., Widenmeyer, M., Niewa, R., & Kraus, F. (2015). On Copper(I)-Fluorides, the Cuprophilic Interaction, the Preparation of Copper Nitride at Room Temperature, and the Formation Mechanism at Elevated Temperatures. *CHEMISTRY: A EUROPEAN JOURNAL*, *21*(8), 3290-3303.
https://doi.org/10.1002/chem.201406136

On Copper(I)-Fluorides, the Cuprophilic Interaction, the Preparation of Copper Nitride at Room Temperature and its Formation Mechanism at Elevated Temperatures**

Patrick Woidy,[a] Antti J. Karttunen,[b] Marc Widenmeyer,[c,‖] Rainer Niewa,[c] Florian Kraus[a,*]

[*,a] Prof. Dr. Florian Kraus, Dipl.-Chem. Patrick Woidy
Fachbereich Chemie
Philipps-Universität Marburg
Hans-Meerwein-Straße 4
35032 Marburg
Fax: +49 (0)6421 28-25676
E-Mail: florian.kraus@chemie.uni-marburg.de
Homepage: http://www.uni-marburg.de/fb15/ag-kraus/

[b] Dr. Antti J. Karttunen
Department of Chemistry
Aalto University
FI-00076 Aalto, Finland

[c] Dr. Marc Widenmeyer, Prof. Dr. Rainer Niewa
Institute of Inorganic Chemistry
University of Stuttgart
Pfaffenwaldring 55
70569 Stuttgart, Germany

[‖] Present Address:
Institute for Materials Science
University of Stuttgart
Heisenbergstraße 3
70569 Stuttgart, Germany

[**] F. K. thanks the Deutsche Forschungsgemeinschaft for a Heisenberg-Professorship at the Philipps-University of Marburg, Solvay Fluor for kind donations of F_2, Prof. Dr. R. Hoppe and Prof. Dr. B. G. Müller, both Giessen, for many chemicals and equipment. We thank B.Sc. Kai Nerkelun for conducting some experiments in aqueous solution. A. J. K. gratefully acknowledges funding from the Alfred Kordelin Foundation, computational resources from the Finnish IT Center for Science (CSC), and helpful discussions with Dr. Silvia Casassa and Dr. Lorenzo Maschio (University of Turin). M. W. and R. N. gratefully acknowledge the assistance of Dr. Thomas Hansen and Alain Daramsy during the *in situ* neutron diffraction experiments at D20 (ILL) as well as the financial support by the Institut Laue-Langevin (ILL, Grenoble) and the Deutsche Forschungsgemeinschaft within the priority program 1415 (SPP1415). Additionally, we thank Dr. Elke Meissner (Fraunhofer Institute for Integrated Systems and Device Technology, Erlangen) for granting measurement time on a thermal analysator in ammonia atmosphere.

Keywords: Fluoride, Nitride, Copper, Liquid Ammonia, Crystal Structures, Cuprophilic Interaction, Neutron Diffraction

Abstract

Our attempts to synthesize the hitherto unknown binary copper(I)-fluoride have led to first successes and a serendipitious result: By conproportionation of elemental copper and copper(II)-fluoride in anhydrous liquid ammonia two copper(I)-fluorides were obtained as simple NH_3 complexes. One of them presents an example of ligand-unsupported “cuprophilic” interactions in an infinite $[Cu_2(NH_3)_4]^{2+}$-chain of alternating Cu−Cu distances. We discovered that both copper(I)-fluorides can easily be converted to Cu_3N at room temperature, just by applying a vacuum. Additionally, we investigated the formation mechanism of the classical synthesis route of Cu_3N starting from CuF_2 and flowing NH_3 in the temperature range between ambient and 290 °C by means of thermal analysis and *in situ* neutron diffraction. The reaction proceeds at elevated temperatures via formation of a blue and amorphous ammoniate $Cu(NH_3)_2F_2$, the reformation of CuF_2 and finally the redox reaction forming Cu_3N.

Introduction

It is common knowledge that copper forms predominantly the oxidation states +I and +II in its compounds. In aqueous solution the oxidation state +II is clearly preferred due to the high hydration enthalpy of the Cu^{2+} cation.[1] So, the disproportionation of Cu(I) to Cu and Cu(II) is thermodynamically favored in aqueous solutions. Traces of O_2 rapidly oxidize Cu(I) to Cu(II) and the colorless solutions become blueish. The copper(I)-halides CuX (X = Cl, Br, I) are easily obtainable from O_2-free aqueous solutions in the form of colorless ("snow white") solids with relatively low solubility by reacting solutions of $CuSO_4$ with NaX(aq) and SO_2 or SO_3^{2-} as a reduction agent.[2] Our attempts to prepare CuF in a similar way only led to a complex mixture of products which neither contained CuF nor Cu and CuF_2.

To the best of our knowledge a binary copper(I)-fluoride is still unknown, however many attempts have been made towards its synthesis. We sum up the current state of the literature to give the reader an impression: The first report on copper(I)-fluoride dates back to Berzelius who reacted a copper(I)-oxide-hydrate with hydrofluoric acid.[3,4] Poulenc reported that he has not been able to reproduce Berzelius' results.[5,6] Instead he obtained a ruby-red copper(I)-fluoride Cu_2F_2 by the reaction of CuCl with HF at temperatures of dark-red glowing heat. This Cu_2F_2 was reported to react with water forming Cu and hydrated CuF_2.[6,7] Ebert and Woitinek reported that CuF was formed as a "directly contacting surface" when compact pieces of Cu were heated in a F_2/Cl_2-mixture at 350 °C.[8] They "unambigously" (see below) assigned their CuF by its powder X-ray pattern to the sphalerite-type. Unfortunately the authors did not report the color of their CuF.

Ruff and coworkers observed that upon oxidation with Cl_2/F_2-mixtures compact Cu forms a CuF-layer which is rapidly oxidized to CuF_2.[9] Von Wartenberg reports that Cu is not attacked by anhydrous HF up to 1200 °C and that slightly below the melting point of CuF_2 red copper(I)-fluoride was formed. In the conproportionation of Cu and CuF_2 at 900-1200 °C he obtained circa 70% of this copper(I)-fluoride in the molten state.[10] Also rapid cooling of this CuF always led to disproportionation, so a further characterization was not possible. The reproduction of Poulenc's works ($CuCl + HF \rightarrow CuF + HCl$) led to a mixture of 4% of red CuF upon solidification, which could not be separated from CuCl by vacuum sublimation.[10] Klemm and coworkers report that the reduction of K_3CuF_6 with H_2 at 300 °C forms Cu(I)-compounds as a red product which is "known for compounds with an overall composition of CuF".[11] Haendler and coworkers heated CuF_2 to 900-1000 °C and could not observe the formation of Cu by powder X-ray patterns at this temperatures. Their findings are thus in contrast to the ones of von Wartenberg. Additionally, the copper fluorides CuF_2 and CuF of Ebert and Woitinek (see above) were shown to be "extremely similar" to Cu_2O and CuCl based on powder X-ray patterns.[12] Crabtree and coworkers report in great detail on various attempts to synthesize CuF – all led only to CuF_2, Cu(OH)F and their hydrates.[13]

By calculations Waddington estimated the lattice energy of CuF assuming the NaCl-structure type with $r(Cu^+) = 0.96$ Å and obtained a formation enthalpy of 11 kcal.[14] Barber and coworkers showed that all monofluorides of the first transition metal period are unstable towards the disproportionation to M and MF_2 (M = transition metal of the first transition metal period). However, CuF was reported having the least instability with ΔH circa −30 kcal/mol.[15] Hoppe noted that no one was successful in preparing pure CuF.[16]

Molecular CuF (and its oligomers) was extensively studied in the gas-phase due to its chemi- and photo-luminescence for chemical lasers. The molecular CuF was obtained by plasma decomposition of CuF_2 (at ca. 10000 K) or by the reaction of Cu with F_2.[17–20]

In recent years the coordination chemistry of CuF was explored: Tris(triphenylphosphane) fluorido copper(I) was obtained from the reaction of CuF_2 with PPh_3 in boiling methanol and structurally characterized in the form of a solvate.[21,22] The Cu(I)-atoms are coordinated by three phosphane ligands and the fluoride ion in a tetrahedron-like arrangement. By X-ray structure analysis the Cu−F-distance was reported to be 2.062(6) Å. IR-spectroscopy on the colorless, powdery compound showed a band at 292 cm^{-1} which was assigned to the Cu−F stretch vibration.[22] All attempts to prepare the monophosphane complex Ph_3PCuF or to cleave off all phosphanes were unsuccessful.[21] $CuF(PPh_3)_3 \cdot 2\,MeOH$ was reported to be stable up to 118 °C. Further warming to 274 °C liberated methanol and triphenylphosphane quantitatively. This was then reported to lead to the formation of "volatile, gaseous" CuF up to 538 °C.[23] A copper(I)-fluoride in the form of a bis(η^2-alkine)-complex was obtained from Cu(I)-thiolates and NBu_4F.[24]

Molecular N_2−Cu−F was shown to be stable in the gas phase,[25] and molecular CuF and *Ng*CuF (*Ng* = Ne, Ar) were observed by Andrews, Riedel and coworkers by matrix spectroscopy.[26] Based on calculations Walsh and coworkers reported the standard formation enthalpy of CuF with −221 kJ/mol with CuF crystallizing in the cinnabarit type (Zinnober, α-HgS) with lattice parameters $a = 3.29$, $c = 9.16$ Å and a Cu−F-distance of 1.85 Å.[27] Furthermore they reported the disproportionation of CuF to CuF_2 and Cu to be exothermic with 49 kJ/mol.

Metallophilicity, especially argento- and aurophilicity, are theoretically and experimentally well established concepts, see for example the seminal works of Jansen,[28,29] Schmidbaur,[30–35] and Pyykkö.[36–41] Besides plenty of literature for theoretical investigations on the topic of cuprophilicity, see for example the literature [37,42–47], less examples of chemical compounds showing this interaction are known. Nearly all have sterically quite demanding, chelating or bridging ligands coordinated to the Cu(I)-atoms, which clearly influences the Cu···Cu-distances as well as their interaction.[48–54]

Examples of compounds with cuprophilic interactions where the ligands are unsupporting are very rare in comparison,[55–59] however the ligands were still quite bulky in these cases. Zheng, Coppens and coworkers reported on an “unstable” $[Cu(NH_3)_2]^+$-dimer which was stabilized in a supramolecular framework,[60] whereas Wagner and coworkers found an equidistant-infinite chain of $[Cu(NH_3)_2]^+$-cations.[61]

Nitrides are an important class of materials and have gained a renewed interest especially in the last decades due to to their application in light emitting diodes, for example GaN. Usually nitrides are synthesized at higher temperatures and pressures,[62] or by thermal decomposition of potentially explosive azides,[63–66] and therefore more energy efficient routes are desired. Feldmann and coworkers have recently reported the synthesis of GaN and CoN in liquid-ammonia-oil-microemulsions at −40 °C,[67–69] highlighting the usefulness of the solvent system to obtain significantly milder temperatures and pressures. Copper(I)-nitride Cu_3N is usually synthesized either from $Cu(NO_3)_2$ and KNH_2 in NH_3 and drying at 160 °C,[70] or more conveniently by passing a flow of NH_3 over CuF_2 at temperatures between 250 and 325 °C.[71] Despite the fact that the latter ammonolysis reaction is known since the 30's of the last century,[71] to the best of our knowledge no information about the reaction sequence is available. Also, a route via the explosive $Cu(N_3)_2$ has been described, which is thermally decomposed to Cu_3N at temperatures up to 185 °C.[64,66,72] Recently, Nakamura and coworkers reported on Cu_3N nanoparticle formation at temperatures between 130 and 200 °C.[73] Cold plasma processes also allow the synthesis of nitrides at quite low temperatures.[74]

Besides our fundamental works on F_2[75,76] and the reaction of fluorides in anhydrous ammonia,[77] we also reported on the diammine silver(I)-fluoride-ammonia(1/2) $[Ag(NH_3)_2]F \cdot 2\,NH_3$.[78] As ammoniates of Ag(I) and Cu(I) may be isotypic,[79] we were hoping to prepare an analogous and eventually also isotypic Cu(I)-fluoride as an ammoniate in order to convert it to the binary CuF. In the following, we report on the preparation of ammine complexes of copper(I)-fluoride. We present a compound featuring infinite $[Cu_2(NH_3)_4]^{2+}$-chains with a shorter Cu−Cu-distance of approximately 2.84 Å and a longer Cu···Cu-distance of circa 3.01 Å, both well in the range of cuprophilic interactions. Finally, we show that Cu_3N can be prepared at room temperature from the ammine complexes of the Cu(I)-fluorides and give an insight into the reaction behavior of CuF_2 in flowing NH_3 at elevated temperatures.

Results and Discussion

A standard route for the synthesis of Cu(I)-halides is the reduction of Cu^{2+} in aqueous solution using SO_2 or SO_3^{2-}. In the presence of X^- (X = Cl, Br, I), the respective Cu(I)-halide is precipitated in the form of a snow-white powder. The analogous reaction of aqueous solutions of $CuSO_4 \cdot 5\ H_2O$, KF and Na_2SO_3, as reducing agent, lead to red-brown precipitates and dark-green solutions. From the solution, after filtration and evaporation of the solvent, $Na_2SO_4 \cdot CuSO_4 \cdot 2\ H_2O$, $Cu_3(SO_4)(OH)_4$, and $K_2Cu(SO_4)_2 \cdot 6\ H_2O$ are obtained and identified by powder X-ray diffraction. Also, other hitherto unidentifiable products are present. The insoluble red-brown product was shown to consist of ill-defined insoluble copper(I/II)-sulfites, such as $Cu_3(SO_3)_2 \cdot Cu_2SO_3 \cdot CuSO_3 \cdot 4\ H_2O$, $Cu_2SO_3 \cdot CuSO_3 \cdot 2\ H_2O$ and $Cu_3(SO_3)_2 \cdot 2\ H_2O$, which are obtained in mixture with compounds such as $Cu_7(OH)_{10}F_4$, $Cu_2(OH)_3F$, $Cu_2O(SO_4)$, $CuO \cdot 3\ H_2O$ and others yet unknown. The aqueous route is clearly and expected not useful for the preparation of Cu(I)-fluorides.

Using anhydrous ammonia instead of water as solvent changes the electrochemical potentials of Cu, Cu(I) and Cu(II). Then, the conproportionation of Cu and Cu(II) to Cu(I) is thermodynamically favored.[79,80] According to equation 1 and scheme 1 and applying the determined constant for the disproportionation, $K_D = 0.044$ L/mol, Cu(I) is the dominating species (> 99%) in solution at concentrations below 0.1 mol/L .[81]

$$2\ Cu^{+}(am) \rightleftharpoons Cu(s) + Cu^{2+}(am) \qquad (1)$$

Therefore, we reacted Cu powder with CuF_2 in anhydrous ammonia and obtained a colorless product (see below) at −40 °C after several weeks of reaction and crystallization time. Despite the reaction being thermodynamically favored, its kinetics is slow, which is however not unexpected. As equation 1 is an equilibrium reaction, the colorless product (see below) is formed among residual red Cu powder and a blue Cu(II)-fluoride-ammoniate with the composition $[Cu(NH_3)_5]F_2 \cdot NH_3$ (**1**). We assume that this Cu(II)-fluoride is formed according to equation 2 (see also scheme 1).

$$CuF_2 + 6\ NH_3 \longrightarrow \underset{\mathbf{1}}{[Cu(NH_3)_5]F_2 \cdot NH_3} \qquad (2)$$

Pentammine copper(II)-fluoride-ammonia(1/1) crystallizes in the shape of blocks in the monoclinic crystal system with space group $P2_1$ and lattice parameters of $a = 7.2711(2)$, $b = 6.0855(1)$, $c = 10.0592(2)$ Å, $\beta = 110.905(3)°$, $V = 415.80(2)$ Å^3, $Z = 2$ at $T = 123$ K. Additional crystallographic details are available from Table 1. The Cu(II)-atom is coordinated by five ammine ligands, the shape of the coordination polyhedron is best described as distorted tetragonal pyramidal (Figure 1a). The four Cu(II)−N-distances of the tetragonal plane are observed in the range from 2.016(1) to 2.049(1) Å, the Cu(II)-N(3)-distance to the "tip" is 2.259(1) Å. Both fluoride ions act as acceptors of eight N−H···F-hydrogen bonds each. So, the fluoride ion F(1) connects four $[Cu(NH_3)_5]^{2+}$-units, and the fluoride ion F(2) bridges three $[Cu(NH_3)_5]^{2+}$-cations. The ammonia molecule of solvation forms three N−H···F-hydrogen bonds, one towards fluoride ion F(1) and two to symmetry equivalent F^--ions of F(2). It is bound to a $[Cu(NH_3)_5]^{2+}$-unit by its free electron pair via an N−H···N-hydrogen bond. By the sum of all hydrogen bonds a three-dimensional network is formed. The unit cell of compound **1** is shown in Figure 1b.

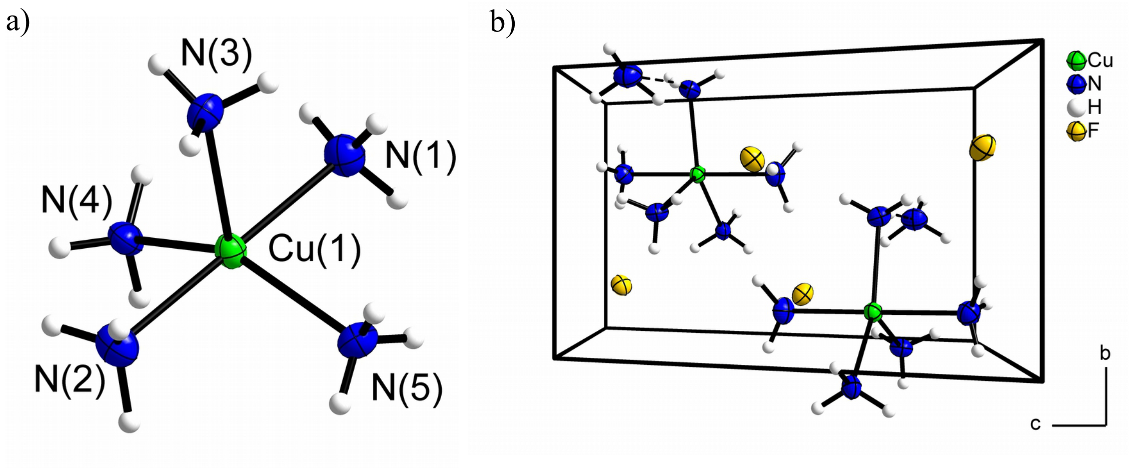

Figure 1. a) The $[Cu(NH_3)_5]^{2+}$-cation, and b) a central projection of the unit cell of $[Cu(NH_3)_5]F_2 \cdot NH_3$ along the *a*-axis. Anisotropic displacement ellipsoids are shown with 70% probability at 123 K, the H-atoms isotropic with arbitrary radii, and the N−H···N-hydrogen bond dashed.

The colorless crystals obtained from the conproportionation are a copper(I)-fluoride with the overall composition $(CuF)_4 \cdot 14\ NH_3$ (**2**), which was shown by X-ray structure analysis on single crystals. Compound **2** crystallizes pseudomerohedraly twinned in the shape of colorless blocks in the monoclinic crystal system with space group *C*2 and the lattice parameters $a = 17.412(3)$, $b = 5.8491(8)$, $c = 10.319(1)$ Å, $\beta = 90.539(9)°$, $V = 1050.9(3)$ Å^3, $Z = 2$ at $T = 123$ K. The assignment of the atom types to the electron densities in the Fourier maps was unequivocally possible by comparison of displacement parameters (N/F) and the standard deviations of atomic distances and angles. Hydrogen atoms on ammine ligands were refined using a riding model, hydrogen atoms on solvate ammonia molecules were located in the difference Fourier map and refined freely. Further crystallographic details are available from Table 1.

Compound **2** is bis(triammine copper(I)) tetraammine dicopper(I) tetrafluoride ammonia(1/4) $\{[Cu(NH_3)_3]_2[Cu_2(NH_3)_4]\}F_4 \cdot 4\ NH_3$, we assume its formation according to equation 3 (see also scheme 1).

$$4\ \mathrm{Cu^{+}(am)} + 4\ \mathrm{F^{-}(am)} + 14\ \mathrm{NH_3} \xrightarrow{-40\ ^{\circ}\mathrm{C}} \underset{\mathbf{2}}{\{[\mathrm{Cu(NH_3)_3}]_2[\mathrm{Cu_2(NH_3)_4}]\}\mathrm{F_4} \cdot 4\ \mathrm{NH_3}} \qquad (3)$$

The $[Cu_2(NH_3)_4]^{2+}$-cation consists formally of two diammine copper(I)-complexes of which the Cu-atoms (Cu(1)−Cu(2)) show a distance of only 2.8394(8) Å to each other (Figure 2a). No bridging or chelating ligands are present between these two Cu atoms. The Cu−N bond lengths of the one moiety are 1.888(4) Å and 1.897(4) Å in the other. The N−Cu−N-angles of 176.0(2) and 174.1(2)°, respectively, are essentially linear and the Cu-atoms of the two $[Cu(NH_3)_2]^{+}$-cations slightly approach each other. The small deviation of the N−Cu−N-angles from 180 ° is due to N−H···F-hydrogen bonding (Figure 2b). The two $[Cu(NH_3)_2]^{+}$-units are tilted by 89.3(2)° and the angles N(1)−Cu(1)−Cu(2) and N(2)−Cu(2)−Cu(1) are 91.98(11) and 92.96(12)°, respectively (Figure 2a). The structure of these $[Cu_2(NH_3)_4]^{2+}$-cations is quite similar to the atom arrangement of [*t*BuCu(CN)Li(OEt$_2$)$_2$],[56,57] and their Cu−Cu-distances are shorter compared to the $[Cu_2(NH_3)_4]^{2+}$-cation (3.0248 Å), which was stabilized by a supramolecular framework.[60] The “intermolecular” Cu···Cu-distance of the formal $[Cu_2(NH_3)_4]^{2+}$-units is elongated to 3.0097(8) Å despite the four fluoride anions bridging them via N−H···F-hydrogen bonds with H···F distances close to 2 Å (Figure 2b). As the N−H···F-hydrogen bond is definitely among the stronger hydrogen bonds, this also adds evidence to a stronger cuprophilic interaction which leads to the shorter Cu−Cu-distances of 2.8394(8) Å. The two ammonia molecules with nitrogen atom N(3), act in a bridging mode – their N−H···F-hydrogen bond is however quite weak with a H···F-distance of approximately 2.6 Å. Thus, these N−H···F-hydrogen bonds may not be responsible for the formation of the shorter Cu−Cu-distance in the formal $[Cu_2(NH_3)_4]^{2+}$-cations.

If additionally a weaker cuprohilic interaction is present for the Cu atoms with a distance of 3.0097(8) Å, an one-dimensional infinite Cu(I)-chain with alternating Cu−Cu-distances is formally obtained (Figure 2a, b). It runs parallel to the crystallographic *b*-axis.

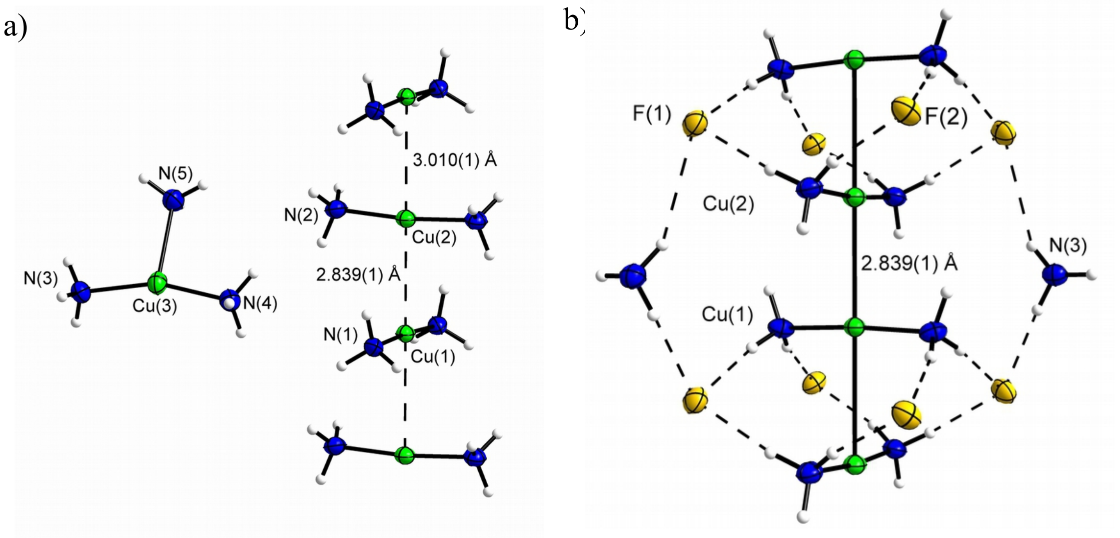

Figure 2. a) A section of the crystal structure of $\{[Cu(NH_3)_3]_2[Cu_2(NH_3)_4]\}F_4 \cdot 4\,NH_3$ showing the coordination sphere of the Cu(I)-cations. b) A central projection showing the N−H···F-hydrogen bonds (dashed) and the coordination of the F^- anions to the $[Cu(NH_3)_2]^+$-cations. Anisotropic displacement ellipsoids are shown with 70% probability at 123 K, the H-atoms isotropic with arbitrary radii.

We investigated the nature of the Cu–Cu-interaction between the $[Cu(NH_3)_2]^+$-units of compound **2** with quantum chemical methods. It is very well known that a proper theoretical description of closed-shell interactions such as the cuprophilic $Cu(d^{10})$−$Cu(d^{10})$-interaction requires electron-correlated post-Hartree-Fock (HF) methods such as MP2 (second-order Møller-Plesset perturbation theory).[37,42,43] Here, we used the local-MP2 (LMP2) method as implemented in the CRYSCOR program package to investigate the cuprophilic interactions (see Experimental for details). Including the complete unit cell of compound **2** in the LMP2 calculations is not necessary to understand the cuprophilic interaction, so we used a one-dimensional $[Cu_2(NH_3)_4]F_2$-polymer extracted from the crystal structure of compound **2** as our model (Figure 3, the rod group of the model is *P*222, the point group is D_2). The presence of the F^--counterions is necessary to balance the charge, as bringing mere $[Cu(NH_3)_2]^+$-units together would result in high coulombic repulsion. In fact, the term "counterion-mediated Cu…Cu bonds" has been coined for short Cu…Cu contact interactions in charged solid-state species.[44]

The relative energy ΔE of the $[Cu_2(NH_3)_4]F_2$ polymer at the Hartree-Fock and LMP2 levels of theory as the function of the Cu–Cu-distance is shown in Figure 3. As we are dealing with a solid polymer composed of charged subunits, it is not possible to calculate the Cu–Cu-interaction energy directly. Instead, we have set the longest studied Cu–Cu-separation of 3.2 Å as the zero level and show how the total energy of the polymer behaves as the $[Cu(NH_3)_2]^+$-units are brought closer to each other. The energies obtained with the HF method show that decreasing the Cu–Cu-distance from 3.2 Å is not energetically favorable (positive ΔE). This is expected, since HF cannot describe metallophilic interactions, leading to repulsion between the monomers.[37] Notably, the electron-correlated LMP2 method shows a very different behavior, as decreasing the Cu–Cu-distance from 3.2 Å is energetically favorable (negative ΔE). The LMP2 energy reaches a minimum at about 2.9 Å, after which the coulombic repulsion between the monomers overcomes the attractive metallophilic interaction and the energy starts to increase. The calculated LMP2 energies thus confirm that there is a cuprophilic Cu(d^{10})−Cu(d^{10})-interaction within compound **2** and the obtained energy minimum at R(Cu–Cu) = 2.9 Å agrees well with the experimentally observed Cu–Cu-distances in the crystal structure (2.839(1) and 3.010(1) Å). ΔE between R = 2.9 and R = 3.2 Å is about 10 kJ/mol and although this cannot be directly interpreted as the Cu–Cu-interaction energy due to the nature of the model, the magnitude of ΔE is in line with previous theoretical investigations on cuprophilic interactions.[42,43]

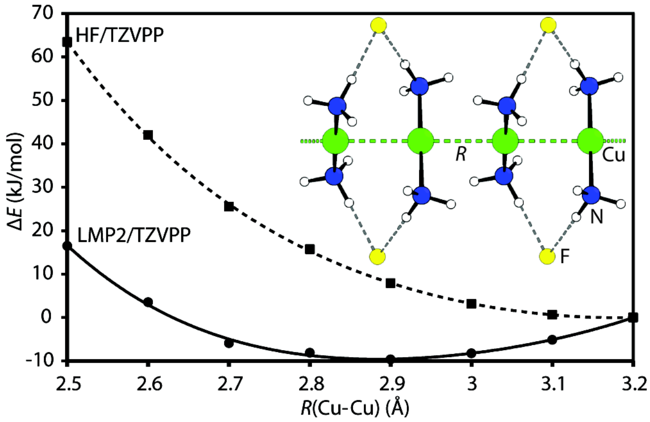

Figure 3. The relative energy ΔE of an idealized one-dimensional [$Cu_2(NH_3)_4$]F_2-polymer at the Hartree-Fock and LMP2 levels of theory as the function of the Cu–Cu-distance. R(Cu–Cu) = 3.2 Å has been set as the zero energy level for both methods (negative ΔE means that the configuration is energetically more favorable than the polymer with R(Cu–Cu) = 3.2 Å). The lines are guides to the eye.

The other Cu(I)-ion (Cu(3)) of the compound is coordinated by three ammine ligands and the Cu−N-distances are 1.936(4), 1.938(4) and 2.257(4) Å, so that one ammine ligand (N(5)) appears to be bound weaker. Therefore, a distorted trigonal coordination sphere around the Cu atom results (Figure 2a). The complex cation is almost planar with a minute deviation of 0.020(3) Å of the atoms from a least-squares plane. The N−Cu−N-angles are 99.91(17), 100.69(17) and 159.36(16)°. Using EXAFS and ^{63}Cu-NMR-spectroscopy, Persson and coworkers investigated the coordination chemistry of Cu(I) in anhydrous ammonia previously and evidenced the [$Cu(NH_3)_3$]$^+$-cation to be the dominating species in solution (in aqueous ammonia the linear [$Cu(NH_3)_2$]$^+$-cation is mainly present).[81] Jacobs and coworkers reported that $[Cu(NH_3)_3]NO_3$, which they could not characterize structurally due to its lability, is isotypic to $[Ag(NH_3)_3]NO_3$.[79] The latter contains however trigonal planar $[Ag(NH_3)_3]^+$-cations due to space group symmetry. To the best of our knowledge compound **2** shows the first direct evidence that triammine complexes of Cu(I) exist not only in anhydrous ammonia solution but also in the solid state. The fluoride ions are embeded in between the cations and form complex N−H···F-hydrogen bond networks. Each F^- anion is surrounded by three $[Cu(NH_3)_3]^+$- and two $[Cu_2(NH_3)_4]^{2+}$-cations, and one molecule of ammonia of solvation. The latter additionally form N−H···N-hydrogen bonds. The unit cell of compound 2 is shown in Figure 4.

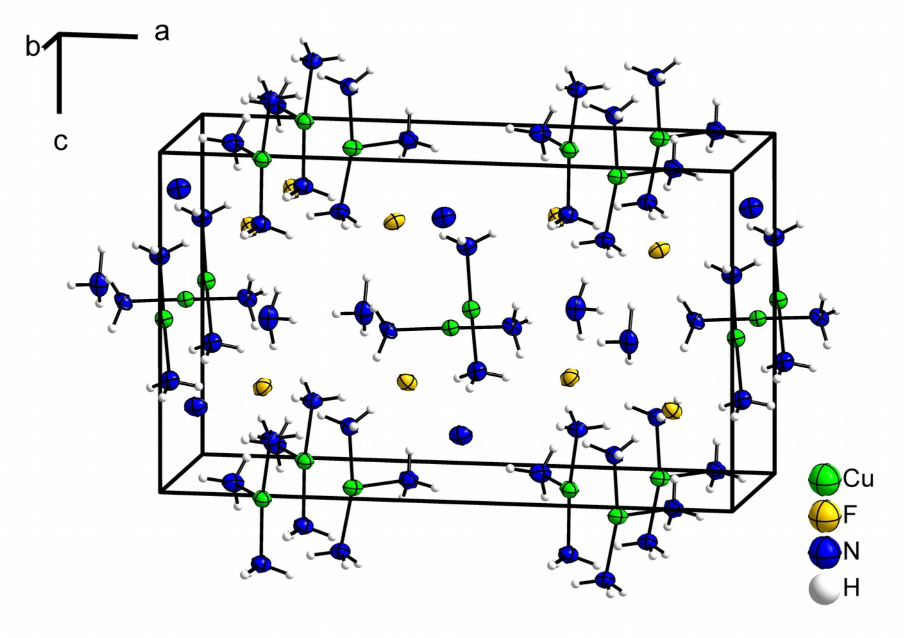

Figure 4. A view of the unit cell of $\{[Cu(NH_3)_3]_2[Cu_2(NH_3)_4]\}F_4 \cdot 4\ NH_3$. Anisotropic displacement ellipsoids are shown with 70% probability at 123 K, the H-atoms isotropic with arbitrary radii.

Compound **2** is only stable at temperatures below approximately −30 °C. Upon warming this $(CuF)_4 \cdot 14\ NH_3$ (which would be formally equivalent to "$CuF \cdot 3.5\ NH_3$") to room temperature, a colorless, microcrystalline powder of the composition $CuF \cdot 3\ NH_3$ (**3**) is formed according to equation 4 (see also scheme 1). Compound **3** can also be obtained directly according to equation 5 (see also scheme 1) within a few days, if Cu and CuF_2 are reacted with NH_3 in a bomb tube at room temperature or at +40 °C. Besides some residual red Cu powder and blue compound **1**, the colorless $CuF \cdot 3\ NH_3$ (**3**) is obtained with the composition of diammine copper(I)-fluoride-ammonia(1/1) $[Cu(NH_3)_2]F \cdot NH_3$, as shown by X-ray structure analysis on single crystals.

$$\underset{\mathbf{2}}{\{[Cu(NH_3)_3]_2[Cu_2(NH_3)_4]\}F_4 \cdot 4\,NH_3} \xrightarrow{+20\text{ °C}} \underset{\mathbf{3}}{4\,[Cu(NH_3)_2]F \cdot NH_3} + 2\,NH_3 \quad (4)$$

$$Cu + CuF_2 + 6\,NH_3 \xrightarrow{+20\text{ bis }+40\text{ °C}} \underset{\mathbf{3}}{2\,[Cu(NH_3)_2]F \cdot NH_3} \quad (5)$$

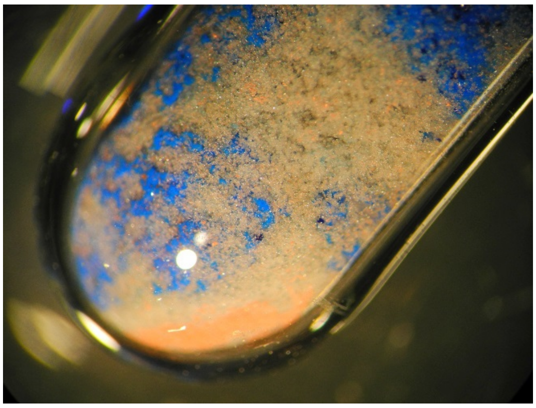

Figure 5. A photograph of the bomb tube containing liquid ammonia, the residual Cu powder (redish), the blue compound **1**, and the colorless compound **3**. Note that the liquid ammonia is colorless, so the solubility of the Cu(II)-species must be very small. This of course further limits the reaction from going to completion.

Figure 5 shows a photograph of the bomb tube after a few days of reaction / crystallization time. Note, that the solution phase is colorless, which indicates that only trace amounts of Cu(II) may be still dissolved, if at all. This confirms the disproportionation constant of Cu(I) described above.

Compound **3** crystallizes in the trigonal crystal system with space group $R3m$ as an inversion twin and the lattice parameters $a = 4.3067(1)$, $c = 19.676(1)$ Å, $V = 316.05(2)$ Å^3, $Z = 3$ at $T = 123$ K. The compound contains a linear diammine copper(I)-cation, of which the Cu(I)−N-distances are observed with 1.86(1) and 1.92(1) Å. The hydrogen atoms of the ammine ligands are in the staggered conformation. The $[Cu(NH_3)_2]^+$-molecules are arranged parallel to the crystallographic *c*-axis. An ammonia molecule of crystallization (N(3)), of which the hydrogen atoms could not be located due to the high symmetry of the Wyckoff position, seems only loosely bound to the Cu(I)-cation with a distance of 2.4865 Å (Figure 6). Formally a two-dimensional infinite layer of trigonal-bipyramidal coordinated Cu(I)-cations is formed. The Cu−F-distance is observed with 4.12(1) Å, so cation and anion may be seen as quite isolated from another. The Cu−Cu-distances are larger than 4 Å, so that in contrast to compound **2** no Cu−Cu-interaction is existent. The fluoride ion acts as an acceptor of N−H···F-hydrogen bonds of six $[Cu(NH_3)_2]^+$-molecules (Figure 7). Three of each are from an upper and lower layer, so that the layers of ammonia of crystallization and $[Cu(NH_3)_2]^+$-cations become interconnected to form a three-dimensional network. Details of the N−H···F-hydrogen bonds are available from the caption of Figure 7. In the latter the unit cell of $[Cu(NH_3)_2]F \cdot NH_3$ (**3**) is shown.

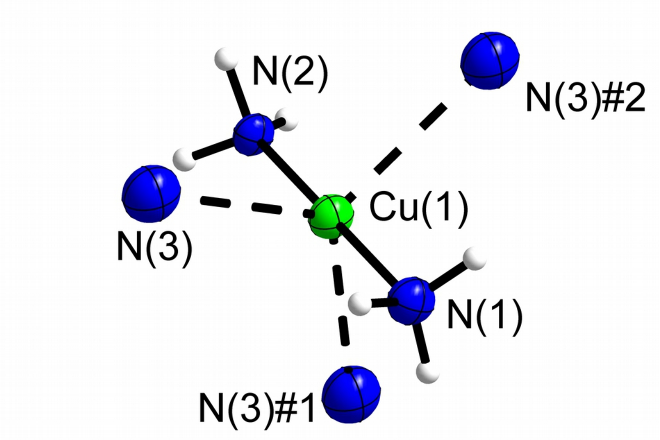

Figure 6. The linear diammine copper(I)-cation of compound **3** and its trigonal coordination (dashed) by ammonia molecules of solvation (N(3)-atoms). Anisotropic displacement parameters are shown at 70% probability at 123 K, H-atoms isotropic with arbitrary radii.

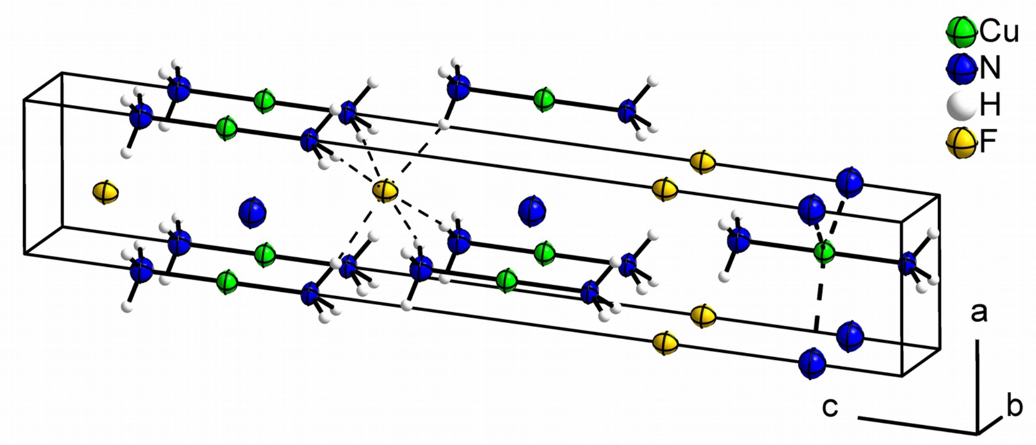

Figure 7. Unit cell of $[Cu(NH_3)_2]F \cdot NH_3$ extended with a $[Cu(NH_3)_2]^+$-molecule to show the acceptor function of the F^--anion by six N−H···F-hydrogen bonds (dashed thin). Anisotropic displacement parameters are shown with 70% probability at 123 K, H-atoms isotropic with arbitrary radii.

Details of N−H···F-hydrogen bonds (Å, °): N(1)−H(1) 0.88(6), H(1)···F(1) 1.99(6), N(1)−F(1) 2.84(1),<N(1)−H(1)···F(1) 161(6); N(2)−H(2) 0.9(1), H(2)···F(1) 2.0(1), N(2)−F(1) 2.86(1), <N(2)−H(2)···F(1) 174(8).

Scheme 1. An overview of the investigated reactions in the system Cu/F/NH_3(liq.).

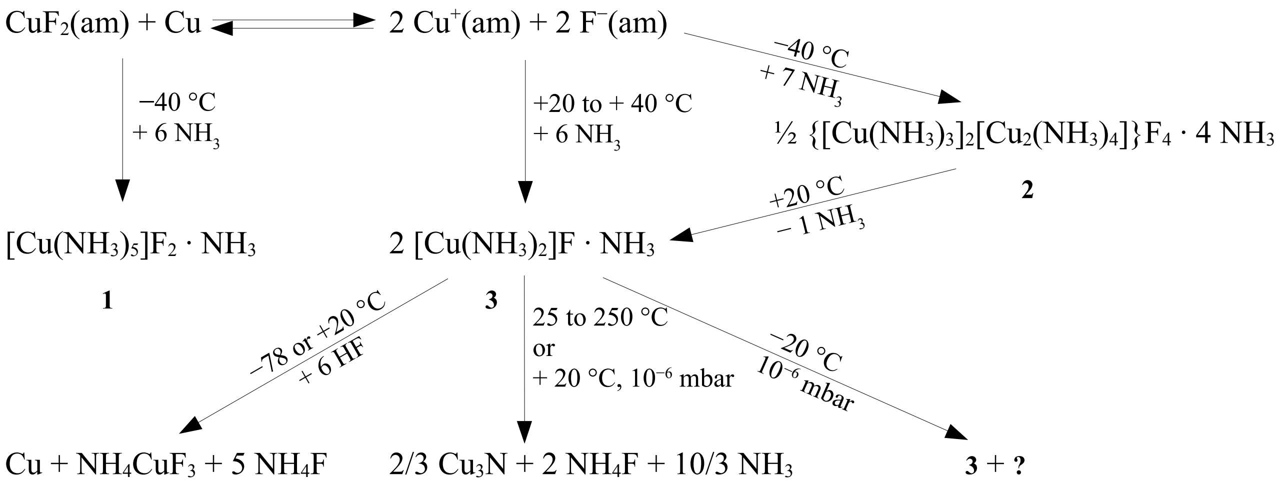

*Investigations on the decomposition behavior of compounds **2** and **3***

Removing crystals of compound **2**, "CuF · 3.5 NH_3", from the cooling and exposing them to air makes the crystals burst immediately due to the rising vapor pressure of ammonia, and the powderous residue becomes blue within a few minutes. This behavior is due to oxidation of Cu(I) by O_2, possibly assisted by moisture, to Cu(II). If crystals of compound **2** are warmed to room temperature under argon, then compound **3**, "CuF · 3 NH_3", seems to be obtained, as a TG/MS-investigation shows identical results as for compound **3** (see below). So, it may be concluded that compound **2** is converted into compound **3** upon warming from −40 °C to room temperature (equation 4, scheme 1). A direct proof is obtained by the powder X-ray patterns: These are essentially identical no matter if compound **3** was made out of compound **2** by heating or by its direct synthesis in a bomb tube (the powder X-ray patterns show besides some elemental Cu also another hitherto unidentified compound in minute amounts). Indexing the powder patterns leads to the trigonal crystal system with lattice parameters $a = 4.3065(4)$, $c = 19.705(2)$ Å, $V = 316.48(6)$ Å^3 at 293 K, which is in well agreement to the lattice parameters of compound **3** determined from its single crystal structure. Compound **3**, $[Cu(NH_3)_2]F \cdot NH_3$, is therefore stable at room temperature and its IR spectrum is shown in Figure 8.

We carried out quantum chemical calculations at the DFT-PBE0/TZVP level of theory to facilitate the assignment of the IR spectrum (see Experimental for details). For the full assignment of the observed modes it is important to interpret the modes arising from the ammine ligands and the solvate ammonia separately. It is also clear that some differences between the predicted and experimental wavenumbers arise especially for the high-energy N–H-stretching modes because we have used an ordered model of compound **3** in space group $P1$ instead of $R3m$. The broad and strong peak centered at 3085 cm^{-1} encompasses both the asymmetric and symmetric N–H-stretching modes of the ammine ligands (calc. wavenumbers of 3231–3149 cm^{-1} are slightly overestimated). The much less intensive higher energy peak at 3209 cm^{-1} arises from the asymmetric N–H-stretching modes of the solvate ammonia (calc. 3389 cm^{-1}), while the symmetric N–H-stretching mode of the solvate ammonia overlaps with the N–H-stretching modes of the ammine ligands (calc. 3164 cm^{-1}). The mode at 1658 cm^{-1} arises from N–H-scissoring of the ammine ligands (calc. 1631 cm^{-1}), while the two less intensive modes between 1550 and 1450 cm^{-1} coincide with the N–H-scissoring of the solvate ammonia (calc. 1562–1517 cm^{-1}). The N–H-wagging modes of the ammine ligands are located at 1367 and 1319 cm^{-1} (calc. 1385 and 1355 cm^{-1}). The peak at 1235 cm^{-1} can be assigned to the N–H-wagging mode of the solvate ammonia (calc. 1109 cm^{-1}). The strong mode at 784 cm^{-1} corresponds to the NH_3-rocking modes of the ammine ligands (calc. 766 cm^{-1}) and the NH_3-rocking mode of the solvate ammonia is observed as a less intense peak at about 650 cm^{-1} (calc. 607 cm^{-1}). It is unclear where the broad band at 2000 cm^{-1} comes from, it might be due to the presence of traces of the decomposition product of compound **1**.

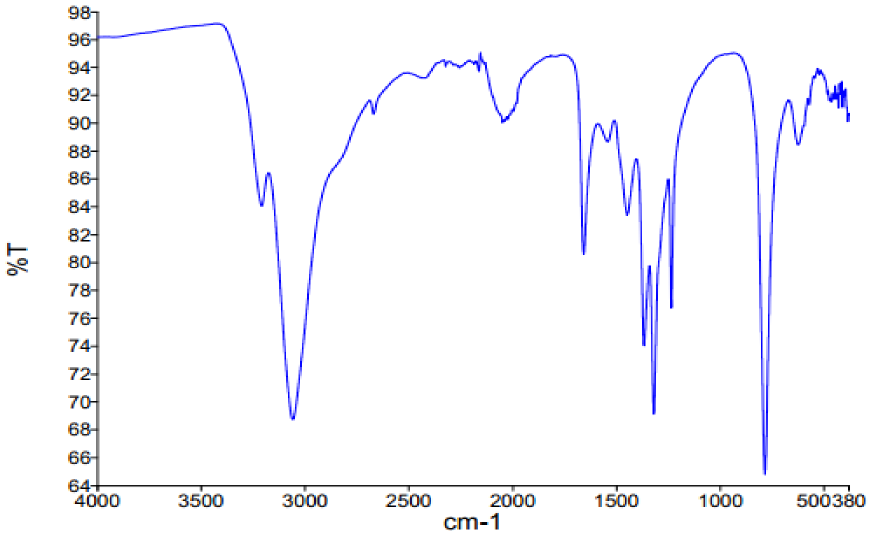

Figure 8: The ATR-IR spectrum of $[Cu(NH_3)_2]F \cdot NH_3$ at room temperature.

When crystals of compound **3** are exposed to (moist) air they neither burst nor deliquesciate, however they also turn blue within a couple of minutes. In the thermogravimetric investigation (Figure 9) three decomposition steps are observed. The mass loss of each step only roughly corresponds to the loss of one mole of NH_3. NH_3 was however mass-spectroscopically detected, besides N_2, at each decomposition step. For the first decomposition step it is plausible to assign it to the loss of the ammonia molecule of crystallization according to equation 6.

$$\underset{\mathbf{3}}{[Cu(NH_3)_2]F \cdot NH_3} \xrightarrow{\text{ca. } 75 - 105\ °\text{C}} „[Cu(NH_3)_2]F“ + NH_3 \qquad (6)$$

Then, in the temperature ranges between 105 – 170 °C and 170 – 230 °C the residual NH_3 ligands and NH_4F are partially expelled.

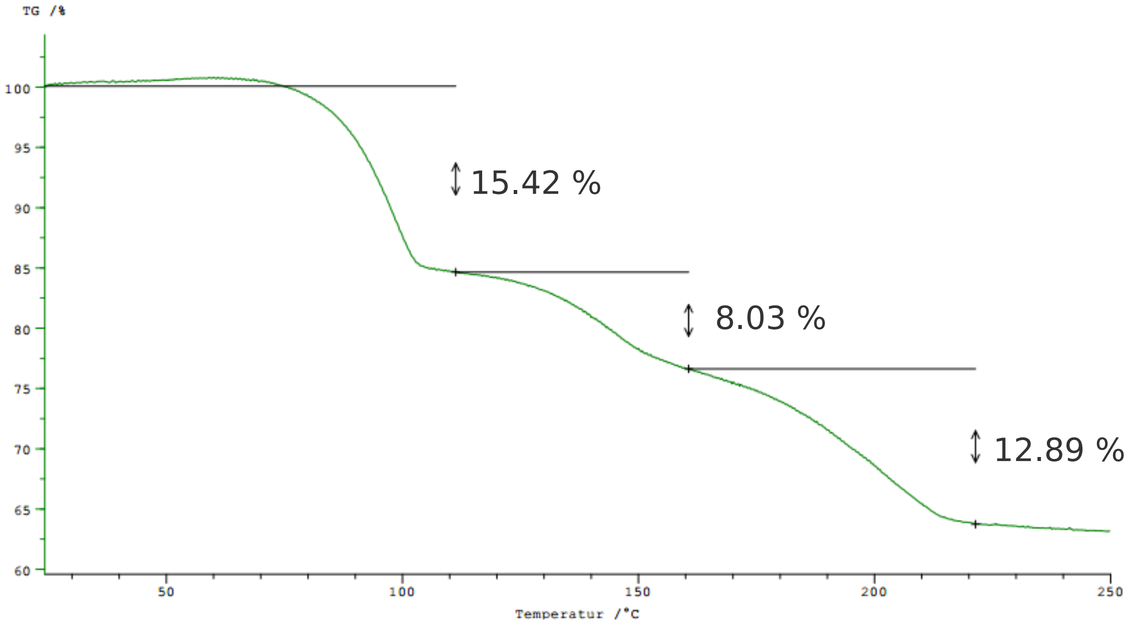

Figure 9: Thermogram of the decomposition of $[Cu(NH_3)_2]F \cdot NH_3$. A mass loss of 12.73% would correspond to the loss of 1 NH_3.

The decomposition product obtained after heating to 250 °C has a dark metallic lustre. The powder X-ray pattern (Figure 10) shows, besides the reflections of metallic Cu likely from the educt, also reflections of copper(I)-nitride Cu_3N, and a hitherto unidentified compound. Reflections of NH_4F are only observed when the decomposition has been carried out in a closed system.

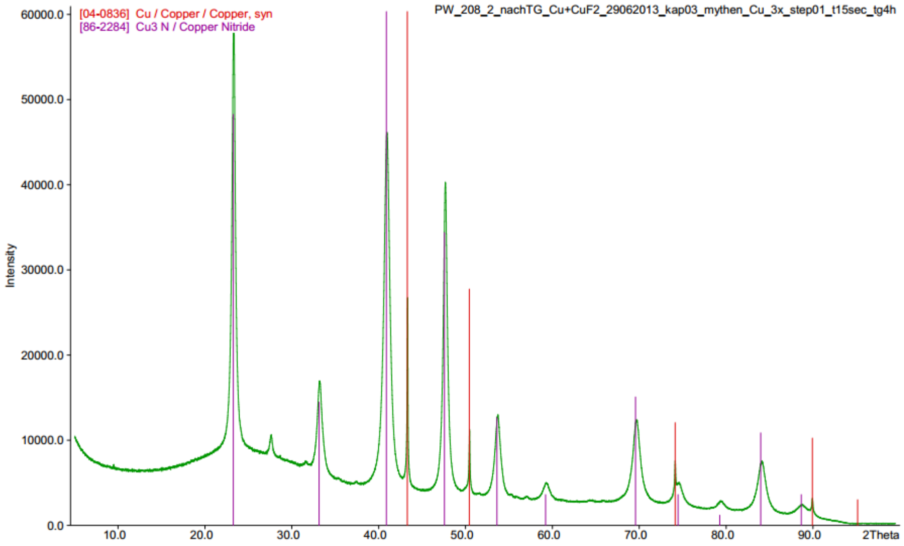

Figure 10: Powder X-ray pattern obtained after the thermal decomposition of $[Cu(NH_3)_2]F \cdot NH_3$.

In the thermal decomposition of compound **3** no copper(I)-fluoride is formed but the metastable copper(I)-nitride Cu_3N is obtained (scheme 1). Presumably the nitride is formed according to equation 7, which would be in agreement with the previously reported formation conditions of Cu_3N from CuF_2 and NH_3 which is starting at circa 270 °C; however, in our case no reduction of Cu(II) to Cu(I) is required.[82,83] Some of the observed metallic copper may also be due to a decomposition of Cu_3N which would explain the mass-spectroscopic observation of traces of N_2.

$$3\,[Cu(NH_3)_2]F \cdot NH_3 \xrightarrow{25-250\,^{\circ}C} Cu_3N + 5\,NH_3 + 3\,NH_4F \qquad (7)$$

3

In a closed system further heating to 500 °C leads to the formation of Cu and CuF_2; in the presence of air Cu, CuF_2, and copper(I)-oxide Cu_2O are obtained.

Attempting to decompose $[Cu(NH_3)_2]F \cdot NH_3$ to the binary CuF by application of a high vacuum of 10^{-6} mbar at room temperature leads to a reaction similar to the one presented in equation 7 and Cu_3N is obtained (Figure 11). Due to its presence in the educt, Cu powder is observed in varying amounts in the powder X-ray patterns. Ammonia, ammonium fluoride and N_2 are pumped off under these conditions.

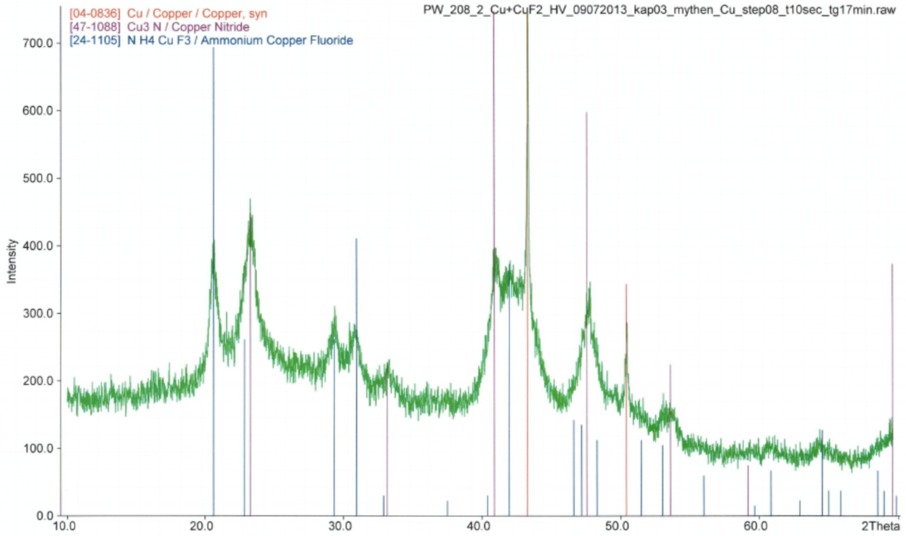

Figure 11: Powder X-ray pattern obtained after decomposing $[Cu(NH_3)_2]F \cdot NH_3$ at room temperature applying high vacuum.

Usually Cu_3N is prepared in a temperature range of 250 – 325 °C from CuF_2 in a stream of NH_3.[71] In our case the NH_4F can be removed in high vacuum at room temperature and Cu_3N is formed under these conditions. So, one may formally assume that the latent instability of a binary CuF, due to the hard-soft combination according to the Pearson concept, is of great aid for the formation of

Cu_3N, which resembles a soft-soft combination. Additionally, our ammine complexes show rather strong N−H···F-hydrogen bonds, which clearly aid in the deprotonation of the ammine ligands.

If compound **3** is exposed for four weeks to high vacuum at temperatures between −20 and −40 °C, its reflexions are still observed in the powder X-ray pattern besides another hitherto unknown compound (scheme 1). Maybe this compound is $[Cu(NH_3)_2]F$. A quantitative decomposition seems thus not possible under these conditions and does not lead to Cu_3N. A decomposition at −80 °C under high vacuum does not proceed at all and not even the ammonia of crystallization is lost from $[Cu(NH_3)_2]F \cdot NH_3$.

Investigations on the reaction behavior of CuF_2 in gaseous NH_3 at elevated temperatures

Elemental copper does not form a compound with ammonia at elevated temperatures, independent of the applied pressure, i. e. if the ammonia is in gaseous, liquid or supercritical state. Still, an interaction is indicated by the transformation of bulk copper into porous material or even semi-fluidical state well below the melting point of copper.[84,85] The origin of this behavior was speculated to be related to the intermediate formation of copper nitride Cu_3N metastable and thus rapidly decomposing under these conditions.

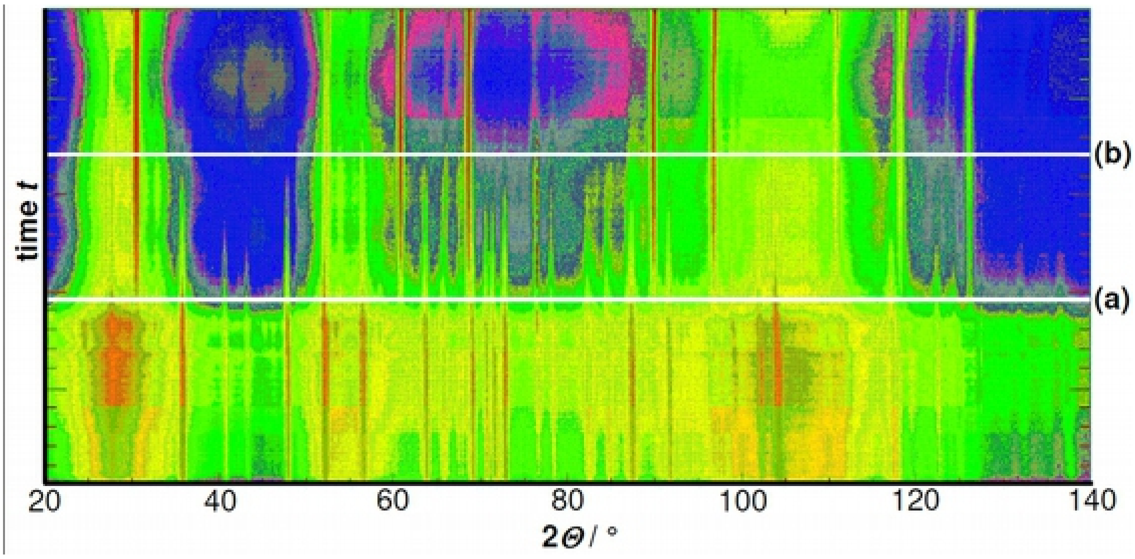

Figure 12:Temperature dependent in situ neutron diffraction data[99] *of the reaction of CuF_2 and flowing NH_3 (λ = 186.802(5) pm, D20, ILL). The intensity is given in false colors on a logarithmic scale. At 284 °C the formation of Cu_3N occur (a). After 148 min at 290 °C single phase $Cu_3N_{0.97(2)}$ is observed (b).*

The interaction of CuF_2 with gaseous ammonia at elevated temperatures to eventually form Cu_3N was investigated via *in situ* neutron diffraction (Figure 12). Immediately after the contact of NH_3

with colorless CuF_2 at ambient temperatures the measurement background is remarkably increased due to the incoherent scattering of the hydrogen atoms of absorbed ammonia molecules and the color changes to blue. Additionally, the temperature increases by approximately 25 K indicating a strongly exothermic reaction. Despite the fact, that only reflections of CuF_2 are observed, we claim the formation of an amorphous ammoniate of CuF_2 (**4**). This assumption is supported by the results achieved from thermal analysis (see below). With increasing the temperature above 120 °C the measurement background slightly starts to decrease indicating a release of ammonia and a decomposition of the formed ammoniate. In analogy to our previous observations during *in situ* investigations on the formation of ε-$Fe_3N_{1\pm x}$ from $FeCl_2$ a complete reformation of CuF_2 was observed at 282 °C.[86] Finally, at 284 °C the formation of Cu_3N starts in perfect accordance to the results observed from a DSC/TG measurement in flowing ammonia. After 148 min at 290 °C CuF_2 was fully converted into $Cu_3N_{0.97(2)}$ according to Rietveld refinements. During the following reaction time no significant change in the composition of Cu_3N was observed. Parallel to the cooling procedure the linear thermal expansion coefficient was determined in the temperature range between 290 °C and 64 °C. A value of $\alpha(Cu_3N) = 5.3(2)\cdot 10^{-6}\ K^{-1}$ was observed in good agreement to the value of $\alpha(Cu_3N) = 6.4(3)\cdot 10^{-6}\ K^{-1}$ determined from powder X-ray diffraction data in the temperature range between –43 °C and –253 °C.[87]

Notably, by using flowing ammonia a complete conversion of CuF_2 into the blue ammoniate **4** was not possible in the temperature range between ambient conditions and 290 °C mainly due to kinetic hindrance effects. Using a stainless steel autoclave at 90 °C CuF_2 reacts in liquid ammonia completely to the blue, but still amorphous ammoniate **4** in the cold zone of the autoclave. The composition of this ammoniate was determined by using a DTA/TG/EGA measurement in helium atmosphere with a heating rate of $1\ K\cdot min^{-1}$. A quite complex and a yet not fully understood multistep decomposition behavior was observed. In summary, two major steps in the TG curve were observed starting at 50 °C and 188 °C with mass losses of 14.3 % and 14.7 %, respectively. Concerning the first step it is assembled of four individual steps with a direct overlap. All changes in the TG curve were accompanied by endothermal peaks in the DTA curve. For all steps a release of ammonia molecules were observed by EGA-MS (m/z = 17, NH_3^+, m/z = 16, NH_2^+, m/z = 15, NH^+) at higher temperatures ($T > 146$ °C). Additionally, a release of water (m/z = 18, OH_2^+) and carbon dioxide (m/z = 44, CO_2^+) was detected originating from impurities such as $CuCO_3$, $Cu(OH)_2$ and $Cu(OH)F$ contained in the commercial CuF_2. Therefore, a larger mass loss was observed then expected ($\Delta m_{\text{exp.}} = 2 \times 12.6$ %) for a release of two ammonia molecules per formula unit from the diammoniate $Cu(NH_3)_2F_2$. The detected impurities were also responsible for a color change to green occurring above 170 °C due to formation of malachite. Summarizing, the composition of the blue and amorphous ammoniate has been determined to $Cu(NH_3)_2F_2$ (**4**) by the use of thermal analysis methods. The reaction sequence of CuF_2 with ammonia at elevated temperatures is depicted in scheme 2.

Scheme 2. An overview of the investigated reactions in the system Cu/F/gaseous NH_3.

$$CuF_2(s) + NH_3\,(g) \xrightleftharpoons[\text{RT,1bar,1h}]{\text{RT,1 bar,1h}} Cu(NH_3)_2F_2\,(\text{amorph.}) \xrightarrow{282\,°C,NH_3} CuF_2 \xrightarrow{284\,°C,NH_3} Cu_3N$$

Chemical Reactions of $[Cu(NH_3)_2]F \cdot NH_3$ and Cu_3N in order to obtain CuF

As the cationic complex $[Cu(NH_3)_2]^+$ reminds of $[Ag(NH_3)_2]^+$, one could argue that its protonation in anhydrous HF (aHF) could set free Cu^+ and thus lead to a precipitate of “CuF” in a similar manner as the soluble $[Ag(NH_3)_2]^+Cl^-$ can be precipitated as AgCl upon addition of $HNO_3(aq)$ from its aqueous solutions.

However, the reactions of $[Cu(NH_3)_2]F \cdot NH_3$ with aHF in a temperature range between room temperature and −78 °C (scheme 1) always led to disproportionation according to equation 8. CuF_2 is also observed according to equation 9 in the mixture of products.

$$2\,[Cu(NH_3)_2]F \cdot NH_3 + 6\,HF \rightarrow Cu + NH_4CuF_3 + 5\,NH_4F \qquad (8)$$

$$NH_4CuF_3 \rightleftharpoons NH_4F + CuF_2 \qquad (9)$$

The reactions of pure Cu_3N with aHF at variuos temperatures between −78 and +20 °C do also not lead to CuF, instead the disproportionation of Cu_3N into Cu, CuF_2, NH_4F, NH_4CuF_3 and one or more yet unknown compounds is observed by powder X-ray diffractometry.

Quantum-chemical calculations on hypothetical CuF structures

Walsh and coworkers have carried out a computational study where they compared the energetics of various hypothetical CuF-structures.[27] By comparing six different bulk CuF-phases (cinnabar, graphite, NiAs, sphalerite, rocksalt, and wurtzite), they found the cinnabar structure incorporating linear F–Cu–F-chains to be the most stable one.

We carried out a comprehensive quantum chemical investigation for 22 hypothetical bulk CuF-phases to understand what kind of structural features are energetically preferable in binary CuF-phases. We optimized the lattice parameters and atomic positions of all studied structures at the DFT-PBE0/TZVP level of theory and also carried out single-point energy calculations at the *ab initio* Local-MP2/TZVPP level of theory (see Experimental for Computational details). The full results of the quantum chemical investigation of the CuF-structures are listed in Tables S1 and S2 in the Supporting information.

With both PBE0/TZVP and LMP2/TZVPP levels of theory, the cinnabar structure (space group $P3_121$) turned out to be energetically the most favorable. The optimized lattice parameter a of the CuF-cinnabar structure (3.25 Å) is in good agreement with the value obtained by Walsh and coworkers at the DFT-PBEsol0/PAW level of theory (3.29 Å), but the value of the lattice parameter c (8.72 Å) is clearly smaller than the one reported (9.16 Å). The energy differences between the CuF-cinnabar structure and the other investigated structures are somewhat smaller than the differences predicted by Walsh and coworkers. For example, we predict the CuF-wurtzite structure to be 3.9 kJ/mol per CuF unit less stable than CuF-cinnabar at the PBE0/TZVP level of theory, while Walsh and coworkers reported an energy difference of 23 kJ/mol per CuF-unit. At the LMP2/TZVPP level of theory the CuF-wurtzite structure is 9.5 kJ/mol per CuF unit less stable than CuF-cinnabar (using the geometry optimized at the PBE0/TZVP level of theory). Considering the fairly large difference between the relative energies predicted by the PBE0/TZVP and LMP2/TZVPP methods, full geometry optimizations with state-of-the-art dispersion-corrected DFT methods (e.g. DFT-PBE0-D3) would be very helpful to confirm the energy ordering of the hypothetical CuF-phases (the D3 dispersion corrections are not yet available in the current version of the CRYSTAL program package).

In addition to optimizing the hypothetical CuF-phases, we also calculated their vibrational spectra. It turned out that the CuF-wurtzite phase with the second lowest relative energy possesses a very low energy vibrational frequency at 8 cm^{-1} that might suggest some structural instability. We displaced the atomic positions of the CuF-wurtzite along the lowest energy vibrational mode and re-optimized the structure without any symmetry constraints. The resulting orthorhombic structure with *Cmcm* space group symmetry no longer shows the low-energy vibrational mode (a = 3.09, b = 5.50, c = 6.38 Å). The optimization leads into clear re-organization of the atomic structure: instead of the tetrahedral bonding in the CuF-wurtzite, the atoms form F–Cu–F-chains in analogy to the CuF-cinnabar structure. However, the structure of the chains is clearly different from CuF-cinnabar as the chains in the CuF-*Cmcm* structure are linear instead of helical (Figure S1, supporting information). At the PBE0/TZVP level of theory, the CuF-*Cmcm* structure is only 1.2 kJ/mol per CuF unit less stable than the CuF-cinnabar structure. At the LMP2/TZVPP level of theory the energy difference is increased to 2.3 kJ/mol per CuF, but the CuF-*Cmcm* structure clearly remains the energetically most favorable CuF-phase after CuF-cinnabar.

The energetically most favorable CuF-cinnabar and CuF-*Cmcm* structures also show the largest band gaps among the investigated CuF phases. The band gap of the CuF-*Cmcm* structure is 2.7 eV and the band gap of the CuF-cinnabar structure is 2.5 eV. The densities of the CuF-cinnabar and CuF-*Cmcm* structures are rather similar (5.126 and 5.023 g/cm^3, respectively) and compared to the other investigated structures their densities are not among the highest or lowest densities. The bonding patterns of the CuF-cinnabar and the CuF-*Cmcm* structures are also similar: both have two shorter Cu–F-bonds (1.95 Å in CuF-cinnabar, 1.92 Å in CuF-*Cmcm*) and four longer ones (2.6–2.7 Å in CuF-cinnabar, 2.79 in CuF-*Cmcm*).

Based on the quantum chemical investigation on the hypothetical CuF-phases, the structures where the Cu atoms are two-coordinated are preferred over higher coordination numbers. Concerning the overall stability of the CuF-cinnabar phase, the disproportionation reaction of CuF-cinnabar to (antiferromagnetic) CuF_2 and Cu turned out to be exothermic by –34 kJ/mol at the DFT-PBE0/TZVP level of theory (Walsh and coworkers obtained a value of –49 kJ/mol). This finding is also in line with the fact that it was not possible to identify any CuF phases during the experimental work, yet.

Conclusion

In the investigated temperature range of −40 to +40 °C, copper and copper(II)-fluoride conproportionate in anhydrous liquid ammonia into the copper(I)-fluorides $(CuF)_4 \cdot 14\,NH_3$ and $CuF \cdot 3\,NH_3$. However these compounds are not fluorido but ammine copper(I) complexes with compositions $\{[Cu(NH_3)_3]_2[Cu_2(NH_3)_4]\}F_4 \cdot 4\,NH_3$ and $[Cu(NH_3)_2]F \cdot NH_3$, respectively. The compound $\{[Cu(NH_3)_3]_2[Cu_2(NH_3)_4]\}F_4 \cdot 4\,NH_3$ contains infinite $[Cu_2(NH_3)_4]^{2+}$-chains, with rather short and alternating Cu−Cu-distances of 2.8394(8) and 3.0097(8) Å. The compound seems to show "cuprophilic" interactions in analogy to the well known "aurophilic" interactions. Warming the compound from −40 °C to room temperature leads to the formation of $[Cu(NH_3)_2]F \cdot NH_3$, in which no Cu−Cu-interactions are present. Further heating to 250 °C – or applying a vacuum at room temperature – transforms $[Cu(NH_3)_2]F \cdot NH_3$ into copper(I)-nitride Cu_3N. To the best of our knowledge we show the first evidence of chemical nitride formation at room temperature (besides the reaction of Li with N_2, and the cold plasma production of Na_3N and Si_3N_4). We assume that it is the latent instability of the binary CuF due to its hard-soft combination according to the Pearson principle, that allows the conversion to the soft-soft Cu_3N under such mild conditions. In the classical "high" temperature synthesis route for Cu_3N the following reaction sequence was observed by combination of *in situ* neutron diffraction and different thermal analysis methods: CuF_2 reacts with ammonia to a blue and amorphous diammoniate $Cu(NH_3)_2F_2$, which at 282 °C completely decomposes under reformation of CuF_2, directly followed by a redox reaction leading to Cu_3N.

Our quantum-chemical calculations on hypothetical CuF structures show that besides a cinnabar-like CuF with helical F−Cu−F-chains, an orthorhombic modification, which is slightly higher in energy and features linear F−Cu−F-chains, would also be feasible.

We predict that the ammine complexes of Cu(I)-fluoride presented here will be of further interest in order to obtain CuF and investigations to reach this target are being continued.

Table 1. Crystallographic details of compounds **1**, **2** and **3**.

	$[Cu(NH_3)_5]F_2 \cdot NH_3$ (1)	**$\{[Cu(NH_3)_3]_2[Cu_2(NH_3)_4]\}F_4 \cdot 4\ NH_3$ (2)**	**$[Cu(NH_3)_2]F \cdot NH_3$ (3)**
Empiric formula	$H_{18}CuF_2N_6$	$H_{42}Cu_4F_4N_{14}$	H_9CuFN_3
Color and habitus	blue blocks	colorless block	colorless blocks
M [g/mol]	203.74	568.64	133.64
Crystal system	monoclinic	monoclinic	trigonal
Space group	$P2_1$	$C2$	$R3m$
a [Å]	7.2711(2)	17.412(3)	4.3067(1)
b [Å]	6.0855(1)	5.8491(8)	$= a$
c [Å]	10.0592(2)	10.319(1)	19.676(1)
β [°]	110.905(3)	90.539(9)	90
V [Å^3]	415.80(2)	1050.9(3)	316.05(2)
Z	2	2	3
ρ_{calc} [Mg/m^3]	1.63	1.80	2.11
λ [Å]		MoK_α, 0.71073	
T [K]		123	
R_{int}, R_σ	0.031, 0.050	0.028, 0.044	0.028, 0.014
$R(F^2)$ (all data), $wR(F^2)$ (all data)	0.034, 0.055	0.056, 0.098	0.029, 0.069
S (all data)	0.973	1.04	1.12
Data, param., con-, restraints	4688, 155, 0, 1	4120, 119, 0, 1	513, 24, 0, 1
Flack x / BASF	0.01(1)	0.02(3)/ 0.22	0.53(4)*
$\Delta\rho_{max}$, $\Delta\rho_{min}$ [eÅ^{-3}]	0.44, −0.65	1.00, −1.38	1.61, −0.99
$(\Delta\sigma)_{max}$	0.001	0.000	0.000

Further details of the crystal structure investigations are available from the Fachinformationszentrum Karlsruhe, D-76344 Eggenstein−Leopoldshafen (Germany), http://www.fiz−karlsruhe.de/icsd.html, on quoting the depository number CSD-428696 for compound **1**, CSD- 428697 for compound **2**, and CSD- 428698 for compound **3**. * refined as inversion twin as no center of symmetry is present.

Experimental Part

All work was carried out excluding humidity and air in an atmosphere of dried and purified argon (Westfalen AG) using high-vacuum glass lines or a glove box (MBraun). Liquid ammonia (Westfalen AG) was dried and stored over sodium (VWR) in a special high-vacuum glass line. All vessels for reactions with liquid ammonia were made out of borosilicate glass and were flame-dried before use. For all experiments using gaseous ammonia flow, ammonia (5.0, Linde) was taken directly from the gas tank.

*Synthesis of $[Cu(NH_3)_5]F_2 \cdot NH_3$ (**1**)*

Pure $[Cu(NH_3)_5]F_2 \cdot NH_3$ is obtained by the reaction of 50 mg (0.5 mmol) CuF_2 and approximately 10 mL liquid ammonia which results in a clear deep-blue solution. After storage at −40 °C deep-blue crystals of compound **1** were obtained. Compound **1** is also obtained as a byproduct in the formation of compounds **2** and **3**. The crystals were separated manually at −40 °C under perfluoroether oil (Galden PFPE, Solvay Solexis) and nitrogen atmosphere. The selected crystals were mounted on the diffractometer by using MicroLoops (MiTeGen) and measured at 123 K.

Synthesis of $\{[Cu(NH_3)_3]_2[Cu_2(NH_3)_4]\}F_4 \cdot 4\ NH_3$ ***(2)***

40 mg (0.4 mmol) CuF_2, 25 mg (0.4 mmol) Cu and approximately 10 mL liquid NH_3 form at −78 °C a clear, deep-blue solution with undissolved Cu remaining. After a crystallization time of several weeks at −40 °C, colorless crystals of compound **2** were obtained from the still blue solution among residual Cu. Single-crystals were selected as described above.

Synthesis of $[Cu(NH_3)_2]F \cdot NH_3$ ***(3)***

A borosilicate glass ampoule was charged with 50 mg (0.5 mmol) CuF_2, 31 mg (0.5 mmol) Cu, and 1 mL NH_3 at −78 °C. After cooling to −196 °C the ampoule was flame sealed, wrapped in paper, and stored at room temperature in a steel vessel. A clear deep-blue solution is obtained which becomes colorless after a few hours of storage at room-temperature. After only a couple of days crystallization time compound **3** is obtained besides some unreacted Cu and compound **1**. Single-crystals were selected as described above.

Synthesis of $Cu(NH_3)_2F_2$ ***(4)***

Approximately 550 mg commercial CuF_2 (99.5 %, Alfa Aesar) were place into a stainless steel autoclave (V4A, Carl Roth, Karlsruhe, Germany) followed by condensation of 38 mL dried ammonia (MC1-702FV gas cleaner, SEAS Pure Gas Inc., San Luis Opispo, USA) by using a tensieudiometer at –78 °C.[88] The reaction mixture was heated at 90 °C for 24 h. After releasing the residual ammonia a blue and amorphous powder was obtained.

Single-crystal X-ray analyses

The X-ray structure analyses were carried out using an Oxford XCalibur3 diffractometer with monochromated molybdenum radiation (MoK_α, $\lambda = 0.71073$ Å) and a CCD-type detector. The evaluation of the diffraction data was carried out using the CRYSALISRED software.[89] An empirical absorption correction was applied using spherical harmonics within SCALE3 ABSPACK. The structures were solved using Direct Methods (SHELXS-97)[90] and refined against F^2 (SHELXL-97)[91] by using SHELXLE.[92] Non-hydrogen atoms were located by Difference Fourier synthesis and refined anisotropically, some were refined using a riding model.

Thermal Investigations

Simultaneous thermogravimetric and differential thermal analyses were carried out with a TG/DT-analyzer SDTQ-600 (TA Instruments, USA) in graphite crucibles under argon. The heating rate was set to 10 °C/min with the sample mass ~20 mg. The mass loss was measured with the precision of 0.1 µg, the DTA sensitivity was up to 0.001 °C. For the DTA/TG/EGA measurements a STA409 with skimmer coupling (Netzsch Gerätebau, Selb, Germany) and a mass spectrometer (Quadstar 422, Pfeiffer Vacuum, Asslar, Germany) operated in helium atmosphere was used. Thermal analysis investigations in ammonia atmosphere were carried out on a STA449C Jupiter (Netzsch) equipped with a corrosion gas setup.

Powder X-ray Diffractometry

Powder X-ray diffraction patterns were obtained on a Stadi-P-Diffractometer (Stoe, Germany) using $Cu_{K\alpha}$ radiation, a germanium monochromator and a Mythen1K detector. The data were handled using the WINXPOW software.[93] The compounds were filled into Lindemann capillaries and flame-sealed.

Powder Neutron Diffraction

The synthesis of Cu_3N was investigated by an *in situ* neutron diffraction experiment using an optimized silica glass measurement cell and the high temperature furnace (HTF) of the D20 (ILL, Grenoble).[94,95] Commercial CuF_2 was reacted in an ammonia flow of 132 $ml \cdot min^{-1}$. The temperature was increased to 120 °C within 1 h and after 1 h at constant temperature within 1 h to 290 °C. After 4 h of annealing at 290 °C the reaction was cooled to ambient conditions with a cooling rate of 5 $K \cdot min^{-1}$.

The *in situ* powder neutron diffraction data were collected at the high flux two-axis powder diffractometer D20 (Institut Laue-Langevin, Grenoble, France) in the range $0° \leq 2\Theta \leq 151°$ (step size $\Delta 2\Theta = 0.1°$) in high resolution mode with a time resolution of $\Delta t_{\min} = 2$ min. A high take-off-angle of 118° from the (115) atomic plane of the Ge monochromator was chosen, resulting in the best average resolution of $\Delta d/d \sim 3 \cdot 10^{-3}$, a high neutron flux at the sample of about $1 \cdot 10^7$ $n \cdot s^{-1} cm^{-2}$ and a nominal wavelength of $\lambda = 188$ pm.[96] The exact determination of the wavelength was performed using a silicon standard (NIST 640b) with corrected unit cell parameters[97] filled into a thin wall vanadium container (outer diameter 6 mm). A wavelength of $\lambda_1 = 186.802(5)$ pm was determined. This value was used during all crystal structure refinements from neutron diffraction data.

The experimental set-up used for the *in situ* investigations is described elsewhere[86,98] in detail. All reaction processes observed by *in situ* neutron diffraction (see Figure 12) are visualized with the

LAMP program available from ILL.[99]

Rietveld Refinements

Rietveld refinements[100,101] of the crystal structures on powder neutron diffraction data were performed using the program *FULLPROF2.k*[102] and pseudo-Voigt functions to describe the reflection profiles. The following parameters are allowed to vary during refinements: The zero point of the 2Θ scale, one scale factor per phase, three reflection widths (Caglioti formula. U, V and W), [103] one mixing (η), two asymmetry parameters, the lattice parameters, the atomic site parameters and the isotropic thermal displacement parameters (B_{iso}). Additionally, an angle dispersive correction (χ) of the mixing parameter was applied. Due to the influence of the gas flow measurement cell the background was treated by interpolation between chosen background points with refinable heights. In case of *ex situ* collected neutron diffraction data in vanadium cylinders the background was described by a polynomial.

IR Spectroscopy

IR spectra of the compounds were recorded under Ar atmosphere by using an ATR-module on a Bruker Alpha FTIR spectrometer and the OPUS software package.[104] Measurements were carried out at room temperature under argon atmosphere and are reported in cm^{-1}.

Computational details

All quantum chemical calculations were carried out using the CRYSTAL14 and CRYSCOR09 program packages.[105–108] In the density functional calculations, we applied the PBE0 hybrid density functional method[109,110] and Gaussian-type, all-electron triple-valence + polarization (TZVP) level basis sets derived from the molecular Karlsruhe def2-TZVP basis sets (see Supporting information for additional basis set details).[111] Default optimization convergence thresholds were applied in all structural optimizations and for the evaluation of the Coulomb and exchange integrals (TOLINTEG), tight tolerance factors of 8, 8, 8, 8, and 16 were used. In the studies on compound **3**, the lattice parameters were kept fixed, while the atomic positions were fully optimized. The H atoms of the solvate ammonia (N3) could not be located in the X-ray crystal structure of **3** (space group $R3m$) and therefore we created an ordered model in the space group $P1$ (structural model included as supporting information). The reciprocal space was sampled using a 6·6·6 Monkhorst-Pack-type k-point mesh (rhombohedral setting, a = 7.014 Å). The harmonic vibrational frequencies were obtained by using the computational scheme implemented in CRYSTAL.[112,113] One imaginary frequency of 80*i,* corresponding to rotational motion of the solvate ammonia, remained in the ordered structural model even after several re-optimizations with tighter convergence thresholds.

For the assignment of the IR spectrum of compound **3**, the harmonic wavenumbers have been scaled by a factor of 0.95 to account for the overestimation typical for *ab initio* harmonic frequencies (see e.g. [114]) In the calculations on hypothetical CuF structures, both the lattice parameters and atomic positions were fully optimized within the symmetry constraints imposed by the space group. The *k*-point meshes used for all studied CuF structures are listed in Supporting Information (e.g. a 12x12x6 mesh was used for the cinnabar structure with $a = 3.246$ Å, $c = 8.724$ Å).

In all LMP2 (local second-order Møller-Plesset perturbation theory) calculations, the preceding CRYSTAL calculations were carried out with very tight TOLINTEG factors of 8, 8, 8, 16, and 50. In the LMP2 calculations on the hypothetical CuF structures, we augmented the TZVP basis set for F with additional polarization functions, increasing the basis set to TZVPP level (the def2-TZVP -based basis set used for Cu corresponds to def-TZVPP level). For the density fitting required in the integral evaluation, we applied basis sets derived from the molecular Karlsruhe RI-MP2 auxiliary basis sets ([115], see Supporting information for additional basis set details). In the case of the CuF structures, the excitation domains of the Wannier Functions were defined by using a Boughton-Pulay criterion with the default value of 0.98 (DOMPUL keyword). We checked that this choice results in consistent excitation domains for the various studied CuF structures. The density-fitting and multipole moment cutoffs d_1 and d_2 were set to 8 and 12 Å, respectively (PAIR keyword). The *k*-point meshes were identical to those applied in the DFT calculations.

For the investigation of the cuprophilic interactions in compound **2** by means of an idealized one-dimensional structure (described in text and included as supporting information), we applied molecular excitation domains (DOMMOL), d_1/d_2 PAIR cutoffs of 8/20 Å, and a 6x1x1 *k*-point mesh (even a much lower d_1/d_2 PAIR cutoff of 6/10 Å results in practically identical energies). Since the LMP2 calculations on the cuprophilic interactions were all based on the infinite 1D polymer structure and no intermolecular energy comparisons for interaction energies were carried out, there was no need to correct for intermolecular basis set superposition error (BSSE). Furthermore, for the closely related aurophilic interaction, the LMP2 method has actually been shown to remove almost all intermolecular BSSE in comparison to canonical MP2.[116]

[1] A. F. Holleman, N. Wiberg, *Lehrbuch Der Anorganischen Chemie*, Walter De Gruyter, Berlin, **2007**.

[2] Georg Brauer, *Handbuch Der Präparativen Anorganischen Chemie*, Enke Verlag, Stuttgart, **1975**.

[3] J. J. Berzelius, *Ann. Phys.* **1824**, *77*, 1–48.

[4] J. J. Berzelius, J.-B. Valerius, *Traité de chimie*, Adolphe Wahlen Et Cie, **1838**.

[5] C. Poulenc, *Compt.rend.* **1893**, *116*, 1446–1449.

[6] C. Poulenc, *Ann. Chim. Phys.* **1894**, *7*, 68–73.

[7] O. Ruff, *Die Chemie Des Fluors*, Julius Springer Verlag, Berlin, **1920**.

[8] H. Woitinek, F. Ebert, *Z. Anorg. Allg. Chem.* **1933**, *210*, 269–272.

[9] O. Ruff, M. Giese, *Z. Anorg. Allg. Chem.* **1934**, *219*, 143–148.

[10] H. von Wartenberg, *Z. Anorg. Allg. Chem.* **1939**, *241*, 381–394.

[11] W. Klemm, E. Huss, *Z. Anorg. Allg. Chem.* **1949**, *258*, 221–226.

[12] H. M. Haendler, L. H. Towle, E. F. Bennett, W. L. Patterson, *J. Am. Chem. Soc.* **1954**, *76*, 2178–2179.

[13] J. M. Crabtree, C. S. Lees, K. Little, *J. Inorg. Nucl. Chem.* **1955**, *1*, 213–217.

[14] A. G. Sharpe, in *Advances in Fluorine Chemistry*, Butterworths Scientific Publications, London, **1960**, pp. 29–67.

[15] M. Barber, J. W. Linnett, N. H. Taylor, *J. Chem. Soc.* **1961**, 3323–3332.

[16] R. Hoppe, *Isr. J. Chem.* **1978**, *17*, 53–59.

[17] S. E. Johnson, P. B. Scott, G. Watson, *J. Chem. Phys.* **1974**, *61*, 2834–2839.

[18] T. C. Ehlert, J. S. Wang, *J. Phys. Chem.* **1977**, *81*, 2069–2073.

[19] R. E. Steele, H. P. Broida, *J. Chem. Phys.* **1978**, *69*, 2300–2305.

[20] U. Naeher, A. Bracker, X. R. Chen, P. Jakob, J. Wanner, *J. Phys. Chem.* **1991**, *95*, 8376–8379.

[21] F. H. Jardine, L. Rule, A. G. Vohra, *J. Chem. Soc. A* **1970**, 238–240.

[22] D. J. Gulliver, W. Levason, M. Webster, *Inorg. Chim. Acta* **1981**, *52*, 153–159.

[23] M. K. Chaudhuri, S. S. Dhar, N. Vijayashree, *Trans. Met. Chem.* **2000**, *25*, 559–561.

[24] K. Köhler, H. Pritzkow, H. Lang, *J. Organomet. Chem.* **1998**, *553*, 31–38.

[25] S. G. Francis, S. L. Matthews, O. K. Poleshchuk, N. R. Walker, A. C. Legon, *Angew. Chem.* **2006**, *118*, 6489–6491.

[26] X. Wang, L. Andrews, F. Brosi, S. Riedel, *Chem. Eur. J.* **2013**, *19*, 1397–1409.

[27] A. Walsh, C. R. A. Catlow, R. Galvelis, D. O. Scanlon, F. Schiffmann, A. A. Sokol, S. M. Woodley, *Chem. Sci.* **2012**, *3*, 2565.

[28] M. Jansen, *Angew. Chem. Int. Ed.* **1987**, *26*, 1098–1110.

[29] M. Jansen, *Angew. Chem.* **1987**, *99*, 1136–1149.

[30] F. Scherbaum, A. Grohmann, B. Huber, C. Krüger, H. Schmidbaur, *Angew. Chem.* **1988**, *100*, 1602–1604.

[31] F. Scherbaum, A. Grohmann, B. Huber, C. Krüger, H. Schmidbaur, *Angew. Chem. Int. Ed.* **1988**, *27*, 1544–1546.

[32] H. Schmidbaur, *Chem. Soc. Rev.* **1995**, *24*, 391–400.

[33] H. Schmidbaur, A. Schier, *Chem. Soc. Rev.* **2012**, *41*, 370–412.

[34] H. Schmidbaur, A. Schier, *Angew. Chem.* **2014**, n/a–n/a.

[35] H. Schmidbaur, A. Schier, *Angew. Chem. Int. Ed.* **2014**, n/a–n/a.

[36] P. Pyykkö, Y. Zhao, *Angew. Chem. Int. Ed.* **1991**, *30*, 604–605.

[37] P. Pyykkö, *Chem. Rev.* **1997**, *97*, 597–636.

[38] P. Pyykkö, N. Runeberg, F. Mendizabal, *Chem. Eur. J.* **1997**, *3*, 1451–1457.

[39] P. Pyykkö, F. Mendizabal, *Chem. Eur. J.* **1997**, *3*, 1458–1465.

[40] P. Pyykkö, *Angew. Chem. Int. Ed.* **2004**, *43*, 4412–4456.

[41] P. Pyykkö, *Angew. Chem.* **2004**, *116*, 4512–4557.

[42] H. L. Hermann, G. Boche, P. Schwerdtfeger, *Chem. Eur. J.* **2001**, *7*, 5333–5342.

[43] E. O'Grady, N. Kaltsoyannis, *Phys. Chem. Chem. Phys.* **2004**, *6*, 680–687.

[44] M. A. Carvajal, S. Alvarez, J. J. Novoa, *Chem. Eur. J.* **2004**, *10*, 2117–2132.

[45] T. Grimes, M. A. Omary, H. V. R. Dias, T. R. Cundari, *J. Phys. Chem. A* **2006**, *110*, 5823–5830.

[46] N. Kuganathan, J. C. Green, *Chem. Commun.* **2008**, 2432–2434.

[47] S. Dinda, A. G. Samuelson, *Chem. Eur. J.* **2012**, *18*, 3032–3042.

[48] J. Beck, J. Strähle, *Angew. Chem.* **1985**, *97*, 419–420.

[49] C.-M. Che, Z. Mao, V. M. Miskowski, M.-C. Tse, C.-K. Chan, K.-K. Cheung, D. L. Phillips, K.-H. Leung, *Angew. Chem.* **2000**, *112*, 4250–4254.

[50] C.-M. Che, Z. Mao, V. M. Miskowski, M.-C. Tse, C.-K. Chan, K.-K. Cheung, D. L. Phillips, K.-H. Leung, *Angew. Chem. Int. Ed.* **2000**, *39*, 4084–4088.

[51] I. I. Vorontsov, A. Y. Kovalevsky, Y.-S. Chen, T. Graber, M. Gembicky, I. V. Novozhilova, M. A. Omary, P. Coppens, *Phys. Rev. Lett.* **2005**, *94*, 193003.

[52] W.-F. Fu, X. Gan, C.-M. Che, Q.-Y. Cao, Z.-Y. Zhou, N. N.-Y. Zhu, *Chem. Eur. J.* **2004**, *10*, 2228–2236.

[53] T. C. Davenport, T. D. Tilley, *Angew. Chem. Int. Ed.* **2011**, *50*, 12205–12208.

[54] F. Schax, C. Limberg, C. Mügge, *Eur. J. Inorg. Chem.* **2012**, *2012*, 4661–4668.

[55] U. Siemeling, U. Vorfeld, B. Neumann, H.-G. Stammler, *Chem. Commun.* **1997**, 1723–1724.

[56] G. Boche, F. Bosold, M. Marsch, K. Harms, *Angew. Chem.* **1998**, *110*, 1779–1781.

[57] G. Boche, F. Bosold, M. Marsch, K. Harms, *Angew. Chem. Int. Ed.* **1998**, *37*, 1684–1686.

[58] S. H. Oakley, M. P. Coles, P. B. Hitchcock, *Inorg. Chem.* **2004**, *43*, 5168–5172.

[59] G. M. Chiarella, D. Y. Melgarejo, A. Rozanski, P. Hempte, L. M. Perez, C. Reber, J. P. J. Fackler, *Chem. Commun.* **2010**, *46*, 136–138.

[60] S.-L. Zheng, M. Messerschmidt, P. Coppens, *Angew. Chem. Int. Ed.* **2005**, *44*, 4614–4617.

[61] G. Margraf, J. W. Bats, M. Bolte, H.-W. Lerner, M. Wagner, *Chem. Commun.* **2003**, 956–957.

[62] C. Braun, M. Seibald, S. L. Börger, O. Oeckler, T. D. Boyko, A. Moewes, G. Miehe, A. Tücks, W. Schnick, *Chem. Eur. J.* **2010**, *16*, 9646–9657.

[63] A. C. Frank, F. Stowasser, H. Sussek, H. Pritzkow, C. R. Miskys, O. Ambacher, M. Giersig, R. A. Fischer, *J. Am. Chem. Soc.* **1998**, *120*, 3512–3513.

[64] L. Grocholl, J. Wang, E. G. Gillan, *Chem. Mater.* **2001**, *13*, 4290–4296.

[65] T. G. Müller, F. Karau, W. Schnick, F. Kraus, *Angew. Chem. Int. Ed.* **2014**, n/a–n/a.

[66] J. Choi, E. G. Gillan, *Inorg. Chem.* **2009**, *48*, 4470–4477.

[67] F. Gyger, P. Bockstaller, D. Gerthsen, C. Feldmann, *Angew. Chem.* **2013**, *125*, 12671–12675.

[68] F. Gyger, P. Bockstaller, D. Gerthsen, C. Feldmann, *Angew. Chem. Int. Ed.* **2013**, *52*, 12443–12447.

[69] F. Gyger, P. Bockstaller, H. Groger, D. Gerthsen, C. Feldmann, *Chem. Commun.* **2014**, *50*, 2939–2942.

[70] E. C. Franklin, *J. Am. Chem. Soc.* **1912**, *34*, 1501–1507.

[71] R. Juza, H. Hahn, *Z. Anorg. Allg. Chem.* **1939**, *241*, 172–178.

[72] J. Choi, E. G. Gillan, *Inorg. Chem.* **2005**, *44*, 7385–7393.

[73] T. Nakamura, H. Hayashi, T. Hanaoka, T. Ebina, *Inorg. Chem.* **2014**, *53*, 710–715.

[74] G. V. Vajenine, *Dalton Trans.* **2010**, *39*, 6013.

[75] J. Schmedt auf der Günne, M. Mangstl, F. Kraus, *Angew. Chem.* **2012**, *124*, 7968–7971.

[76] J. Schmedt auf der Günne, M. Mangstl, F. Kraus, *Angew. Chem. Int. Ed.* **2012**, *51*, 7847–7849.

[77] F. Kraus, *BioInorg. React. Mech.* **2012**, *8*, DOI 10.1515/irm-2012-0003.

[78] F. Kraus, S. A. Baer, M. B. Fichtl, *Eur.J.Inorg.Chem.* **2009**, 441–447.

[79] U. Zachwieja, H. Jacobs, *Z.Anorg.Allg.Chem.* **1989**, *571*, 37–50.

[80] V. Doetsch, J. Jander, U. Engelhardt, C. Lafrenz, J. Fischer, H. Nagel, W. Renz, G. Türk, T. von Volkmann, G. Weber, *Chemistry in Nonaqueous Ionizing Solvents - Volume I Chemistry in Anhydrous Liquid Ammonia - Part 1 Anorganische Und Allgemeine Chemie in Flüssigem*

Ammoniak, Friedr. Vieweg & Sohn, Braunschweig, **1966**.
[81] K. B. Nilsson, I. Persson, *Dalton Trans.* **2004**, 1312–1319.
[82] R. Juza, H. Hahn, *Z. Anorg. Allg. Chem.* **1938**, *239*, 282–287.
[83] A. Wosylus, U. Schwarz, L. Akselrud, M. G. Tucker, M. Hanfland, K. Rabia, C. Kuntscher, J. von Appen, R. Dronskowski, D. Rau, et al., *Z. Anorg. Allg. Chem.* **2009**, *635*, 1959–1968.
[84] G. T. Beilby, G. G. Henderson, *J. Chem. Soc., Trans.* **1901**, *79*, 1245–1256.
[85] B. Hertweck, S. Zhang, T. G. Steigerwald, N. S. A. Alt, R. Niewa, E. Schluecker, *Chem. Eng. Technol.* **2014**, *37*, 1835–1844.
[86] M. Widenmeyer, T. C. Hansen, E. Meissner, R. Niewa, *Z. Anorg. Allg. Chem.* **2014**, *640*, 1265–1274.
[87] D. Rau, Technische Universität München, **2012**.
[88] G. F. Hüttig, *Z.Anorg.Allg.Chem.* **1920**, *114*, 161–173.
[89] Oxford Diffraction, *CrysalisRED*, Oxford Diffraction, UK, **2008**.
[90] G. M. Sheldrick, *SHELXS-97*, Göttingen, **1997**.
[91] G. M. Sheldrick, *SHELXL-97*, Göttingen, **1997**.
[92] C. B. Hübschle, G. M. Sheldrick, B. Dittrich, *Journal of Applied Crystallography* **2011**, *44*, 1281–1284.
[93] *STOE WinXPOW*, Stoe & Cie GmbH, Darmstadt, **2011**.
[94] M. Widenmeyer, R. Niewa, H. Kohlmann, Institut Laue-Langevin (ILL), **2013**.
[95] M. Widenmeyer, R. Niewa, T. C. Hansen, H. Kohlmann, *Z. Anorg. Allg. Chem.* **2013**, *639*, 285–295.
[96] T. C. Hansen, P. F. Henry, H. E. Fischer, J. Torregrossa, P. Convert, *Meas. Sci. Technol.* **2008**, *19*, 034001.
[97] D. Yoder-Short, *J. Appl. Cryst.* **1993**, *26*, 272–276.
[98] M. Widenmeyer, T. C. Hansen, R. Niewa, *Z. Anorg. Allg. Chem.* **2013**, *639*, 2851–2859.
[99] *LAMP, the Large Array Manipulation Program, Version 8.1*, **2013**.
[100] H. M. Rietveld, *Acta Crystallogr.* **1967**, *22*, 151–152.
[101] H. M. Rietveld, *J. Appl. Cryst.* **1969**, *2*, 65–71.
[102] J. Rodríguez-Carvajal, *FULLPROF 2.k*, ILL-JRC, **2012**.
[103] G. Caglioti, A. Paoletti, F. P. Ricci, *Nucl. Instrum.* **1958**, *3*, 223–228.
[104] *OPUS*, Bruker Optik GmbH, Ettlingen, **2009**.
[105] R. Dovesi, R. Orlando, A. Erba, C. M. Zicovich-Wilson, B. Civalleri, S. Casassa, L. Maschio, M. Ferrabone, M. De La Pierre, P. D'Arco, et al., *Int. J. Quantum Chem.* **2014**, n/a–n/a.
[106] R. Dovesi, V. R. Saunders, R. Roetti, R. Orlando, C. M. Zicovich-Wilson, F. Pascale, B. Civalleri, K. Doll, N. M. Harrison, I. J. Bush, et al., *CRYSTAL14 User's Manual*, University Of Torino, Torino, **2014**.
[107] C. Pisani, L. Maschio, S. Casassa, M. Halo, M. Schütz, D. Usvyat, *J. Comput. Chem.* **2008**, *29*, 2113–2124.
[108] C. Pisani, M. Schütz, S. Casassa, D. Usvyat, L. Maschio, M. Lorenz, A. Erba, *Phys. Chem. Chem. Phys.* **2012**, *14*, 7615–7628.
[109] J. P. Perdew, K. Burke, M. Ernzerhof, *Phys. Rev. Lett.* **1996**, *77*, 3865–3868.
[110] C. Adamo, V. J. Barone, *J. Chem. Phys.* **1999**, *110*, 6158–6170.
[111] F. Weigend, R. Ahlrichs, *Phys. Chem. Chem. Phys.* **2005**, *7*, 3297–3305.
[112] F. Pascale, C. M. Zicovich-Wilson, F. Lopez, B. Civalleri, R. Orlando, R. Dovesi, *J. Comput. Chem.* **2004**, *25*, 888–897.
[113] C. M. Zicovich-Wilson, F. Pascale, C. Roetti, V. R. Saunders, R. Orlando, R. Dovesi, *J. Comput. Chem.* **2004**, *25*, 1873–1881.
[114] A. P. Scott, L. Radom, *J. Phys. Chem.* **1996**, *100*, 16502–16513.
[115] F. Weigend, M. Häser, H. Patzelt, R. Ahlrichs, *Chem. Phys. Lett.* **1998**, *294*, 143–152.
[116] N. Runeberg, M. Schütz, H.-J. Werner, *J. Chem. Phys.* **1999**, *110*, 7210–7215.